Audiovisual time-to-collision estimation for accelerating vehicles: The acoustic signature of electric vehicles impairs pedestrians' judgments

Marlene Wessels[1,*], Sophie Kröling[2], Daniel Oberfeld[1]

1 Institute of Psychology, Section Experimental Psychology, Johannes Gutenberg-Universität Mainz, Wallstrasse 3, 55122 Mainz, Germany
2 German Insurers Accident Research (UDV), Wilhelmstr. 43 /43 G, 10117 Berlin, Germany
** Contact author: mwessels@uni-mainz.de*

Abstract

To avoid collisions, pedestrians intending to cross a road need to accurately estimate the time-to-collision (TTC) of an approaching vehicle. For TTC estimation, auditory information can be considered particularly relevant when the approaching vehicle accelerates. The sound of vehicles with internal combustion engine (ICEVs) provides characteristic auditory information about the acceleration state (increasing speed and engine load). However, for electric vehicles (EVs), the acoustic signature during acceleration is less salient. Although the auditory detection of EVs has been studied extensively, there is no research on potential effects of the altered acoustic signature of EVs on TTC estimation. To close this gap, we compared TTC estimates for ICEVs and for EVs with and without active acoustic vehicle alerting system (AVAS). We implemented a novel interactive audiovisual virtual-reality system for studying the human perception of approaching vehicles. Using acoustic recordings of real vehicles as source signals, the dynamic spatial sound field corresponding to a vehicle approaching in an urban setting is generated based on physical modeling of the sound propagation between the vehicle and pedestrian (listener) and presented via sound field synthesis (higher-order Ambisonics). In addition to the auditory simulations, the scene was presented visually on a head-mounted display with head tracking. Participants estimated the TTC of vehicles either approaching at a constant speed or accelerating positively. In conditions with constant speed, TTC estimates for EVs with and without AVAS were similar to those for ICEVs. In contrast, for accelerating vehicles, there was a substantial effect of the vehicle type on the TTC estimates. For the EVs, the mean TTC estimates showed a significant overestimation. Thus, subjects on average perceived the time of arrival of the electric vehicle at their position as longer than it actually was. The extent of overestimation increased with the acceleration and with the presented TTC. This pattern is similar to a first-order TTC estimation representing a failure to consider the acceleration, which is also consistently reported in the literature for visual-only presentations of accelerating objects. In comparison, the overestimation of TTC was largely reduced for the accelerating ICEVs. The AVAS somewhat improved the TTC estimates for the accelerating EVs, but without reaching the same level of accuracy as for the ICEVs. In real traffic scenarios, overestimations of the TTC of approaching vehicles might lead to risky road-crossing decisions. Therefore, our finding that pedestrians are significantly less able to use the acoustic information emitted by accelerating EVs for their TTC judgments, compared to accelerating ICEVs, has important implications for road traffic safety and for the design of AVAS technologies.

Introduction

Safe mobility requires the ability to avoid collisions with objects in the environment. Especially pedestrians are vulnerable road users, for whom a collision represents a hazard with potentially devastating consequences. In fact, more than 400,000 pedestrians are killed in road traffic each year worldwide (International Transport Forum, 2012). The majority of pedestrian accidents occurred in urban areas, most of them during road-crossings. Thus, it is of particular relevance for pedestrians to avoid collisions, when crossing the road in front of an approaching vehicle. In Germany, the most frequent human cause of pedestrian accidents with personal injury is pedestrians' improper behavior when crossing the road, such as, not paying attention to road traffic (Statistisches Bundesamt, 2021). In this context, the important role of hearing becomes evident, because auditory features of the vehicles provide relevant information to pedestrians, even when not looking at the traffic. In the course of the mobility change, however, the question arises whether and to what extent the acoustic signature of electric vehicles (EVs), which is significantly altered compared to conventional vehicles with an internal combustion engine (ICEVs), impairs the perception of pedestrians. The altered acoustic signature of EVs might pose a potential risk and is therefore subject of the present study.

To cross the road safely in front of an approaching vehicle, the time remaining until the vehicle arrives at the pedestrian's position (time-to-collision, TTC[1]) must be longer than the time required to cross. Thus, pedestrians need to estimate the TTC as accurately as possible to adjust their crossing behavior. For TTC estimation, various visual cues as well as auditory information can be used (e.g., DeLucia et al., 2016; Jenison, 1997; Schiff & Oldak, 1990). However, the impact of auditory information on TTC estimation has been investigated in only a limited number studies, which reported largely consistent results (DeLucia et al., 2016; Hofbauer et al., 2004; Keshavarz et al., 2017; Prime & Harris, 2010; Wessels et al., under review; Zhou et al., 2007).

For instance, DeLucia et al. (2016) and Keshavarz et al. (2017) presented objects approaching the observers on a collision course at constant velocities, in three different conditions – auditory-only, visual-only, and audiovisual. In principle, heuristic object features as well as more reliable cues were available in the auditory and visual modality and could therefore be used for TTC estimation. Auditory heuristic-based cues included, for example, the sound pressure level of the object at the moment of estimation. In contrast, more reliable auditory information about the object's TTC was provided by the relative rate of change of the sound pressure. However, auditory heuristic-based cues contributed more strongly to auditory TTC estimation than the available more reliable auditory information. In contrast, the weighting of heuristic cues and more reliable information was shifted towards the latter in visual TTC judgments. When both visual and auditory information of an approaching object were available, humans relied more strongly on visual than on auditory information. The mean TTC estimates in the audiovisual condition were more similar to those in the visual condition, but differed from those of the auditory condition. DeLucia et al. (2016) concluded that for object approaches at a constant velocity, additional sound did not play a major role in TTC estimation. Therefore, we would not expect the acoustic signature of an EV to affect audiovisual TTC estimates differently than the sound of an ICEV at a constant velocity.

However, we recently showed for the first time that auditory information is of high relevance in TTC estimation for accelerating objects (Wessels et al., under review). Formally, the TTC for constantly accelerating objects at a given point in time t depends on the vehicle's instantaneous distance D, velocity v as well as its constant acceleration a, so that $TTC(t) = \frac{-v(t) + \sqrt{2a\,\mathrm{D}(t) + v(t)^2}}{a}$. Hence, to accurately estimate the TTC of an accelerating object, both its velocity and acceleration have to be considered during estimation. Previous studies on TTC estimation for visually

[1] Note that, for reasons of simplicity, we use the term "time-to-collision" even when the vehicle is not on a direct collision with the simulated observer, so that strictly speaking the term "time-to-passage" would be more appropriate.

presented accelerating objects have indicated significant estimation errors (e.g., Benguigui et al., 2003; Benguigui & Bennett, 2010; Bennett & Benguigui, 2016; Kaiser & Hecht, 1995; Lee et al., 1983; Rosenbaum, 1975; Senot et al., 2003). The studies show rather consistently that humans have difficulty to adequately account for the acceleration of an object in their TTC estimates. Instead, they estimate the TTC of an accelerating object as if it were moving at a constant velocity. If the velocity, but not the acceleration is considered in TTC estimation, this results in a so-called first-order TTC estimation (Tresilian, 1995), which is related to the actual TTC as $TTC1(t) = TTC(t) + \frac{a \cdot TTC^2(t)}{2v(t)}$. Thus, the first-order TTC estimate TTC1 exceeds the actual TTC for a positively accelerating object, and corresponds to an overestimated TTC. That is, the object is estimated to take longer to travel from one position to another than it is actually the case, because the increase in velocity across time is ignored. The difficulty to consider a visually presented acceleration in TTC estimation might result from a relatively low sensitivity to visual acceleration (e.g., Gottsdanker et al., 1961; Snowden & Braddick, 1991; Watamaniuk & Heinen, 2003; Werkhoven et al., 1992). Hence, the acceleration must be relatively strong to be visually detected (Werkhoven et al., 1992), and presumably to be considered in TTC estimation. An overestimated TTC implies that a pedestrian could decide to cross the street in front of an approaching vehicle, even though the time remaining until the vehicle arrives at her or his position might be shorter than the time needed to safely cross the street. Hence, TTC overestimation poses a serious collision risk in a real traffic scenario. Therefore, it is of high practical relevance to identify influential factors that condition or counteract a first-order estimation for accelerating vehicles to increase pedestrian safety.

In our study that investigated the effects of auditory information on TTC estimation for accelerating objects (Wessels et al., under review), we presented approaching vehicles that either travelled at a constant velocity or accelerated, in a visual-only and in an audiovisual presentation condition. Participants estimated the TTC of the vehicles from the perspective of a pedestrian standing at the curb. Consistent with the literature, the TTC estimates for the accelerating vehicles in the visual-only condition were similar to a first-order pattern, showing a pronounced overestimation of the TTC that increased with the actual TTC. In contrast, when the vehicle sound was added in the audiovisual condition, this effect was largely removed. The mean TTC estimates were close to the actual TTCs and thus significantly more accurate compared to the visual-only condition. For constant velocities, participants estimated the TTC in both presentation conditions mostly accurately. Taken together, the vehicle sound was found to play a major role in TTC estimation for accelerating, but not in constant-velocity object approaches.

In the study outlined above, we presented the sound of a conventional ICEV. For this vehicle type, the sound emitted during acceleration is particularly salient because the sound spectrum of an ICEV shifts to higher frequencies as the engine speed increases, and the sound level rises as the engine load increases (Zeller, 2018). We therefore suggested that the sound profile conveyed characteristic acceleration cues that were unavailable visually and likely familiar to the participants, which might have increased the sensitivity to acceleration. The results of Wessels et al. (under review) thus pose the question of whether TTC estimates for accelerating EVs could be significantly less accurate than for ICEVs, because acoustic cues to acceleration are less salient for EVs than for ICEVs. EVs are generally quieter than ICEVs (Gergen et al., 2012; Oberfeld et al., under review; Poveda-Martínez et al., 2017), and more importantly the sound profile of an EV misses distinct auditory cues such as audible gear changes, which clearly indicate a change in speed in ICEVs. In addition, the powertrain noise of an EV is currently less familiar to most people. If the acceleration-related sound changes are substantially less salient for an EV than for an ICEV, it is conceivable that an acceleration of an EV might be more difficult to detect and to consider than that of an ICEV. Thus, an EV's acceleration might not be as adequately accounted for in TTC estimation as the acceleration of an ICEV. As a result, TTC estimates for accelerating EVs might resemble a first-order pattern, i.e., reflect an overestimation of TTC that is most pronounced at a high acceleration level, a long actual TTC, and a low instantaneous speed at the moment of estimation. Under these conditions, we would also expect the largest deviations from the TTC

estimates for an accelerating ICEV, which we expect to be close to the actual TTC values based on our previous study.

To ensure the auditory detectability of EVs at low velocities and thus increase the safety of vulnerable road users, legislative measures have been taken that mandate the implementation of acoustic vehicle altering systems (AVAS) in EVs (NHTSA 141, 2018; UNECE R138, 2017). The European legislation UNECE R138 requires that the AVAS emit artificial sound to the outside world up to a speed of at least 20 km/h, with a minimum sound level of 56 dB(A) and a maximum of 75 dB(A) at 20 km/h, which is similar to the level of an ICEV. Recent studies showed that EVs with AVAS (EVs+AVAS) can be detected comparably well as louder ICEVs when they travel at a constant velocity (e.g., Parizet et al., 2014; Poveda-Martínez et al., 2017). Since the AVAS is also required to signal the speed modulation by changes in frequency, it potentially provides information about the vehicle's deceleration and acceleration. An active AVAS might therefore improve the sensitivity to acceleration and thus enhance the consideration of acceleration during TTC estimation, compared to an EV without AVAS.

For this reason, the present study was designed to investigate whether and to what extent TTC estimates for accelerating vehicles differ between ICEVs, EVs without AVAS, and EVs with AVAS. Using an audiovisual urban traffic simulation, we presented the three vehicle types at various constant velocities, but most importantly also during acceleration. Participants estimated the TTC of the vehicles from a pedestrian's perspective. For constant-velocity approaches, we expected no significant differences between the TTC estimates for the different vehicle types. In contrast, we hypothesized an effect of vehicle type for accelerated vehicle approaches. More precisely, we expected the TTC estimates for the accelerating EVs without AVAS to be similar to a first-order pattern, i.e., an overestimated TTC that increases with acceleration and actual TTC, but decreases with velocity. In opposition, the estimates for the accelerating ICEV should be comparatively accurate, so that the influence of acceleration level, actual TTC and velocity is substantially reduced. In line with the deviations between first-order estimates and actual TTCs, we hypothesized that the differences between the estimates for accelerating EVs without AVAS and ICEV would be most pronounced at low velocities, high levels of acceleration and long actual TTCs. Finally, we expected the AVAS to have a positive effect, so that the TTC estimates for the accelerating EV with AVAS would show a less pronounced first-order pattern than those for the EV without AVAS.

Methods

In the present study, we used a state-of-the-art audiovisual virtual reality (VR) simulation system and stimuli previously described in greater detail in a study by Oberfeld et al. (under review).

Design and implementation of the audio-visual VR simulation system

We designed and implemented a high-performance interactive audiovisual VR system to investigate the audiovisual perception of approaching vehicles. The tire noise emitted by a vehicle as well as the aerodynamic noise dynamically depend on the velocity (e.g., Kropp et al., 2012). The powertrain noise depends on engine speed and engine load, which, in turn, depend on factors like the selected gear, acceleration, road inclination, etc. Since we were not aware of completely convincing approaches for the simulation of tire, powertrain and aerodynamic noise in dynamic driving situations with changing speed, acceleration, and load conditions, the auditory stimuli were based on acoustic recordings of real vehicles on a test track, which were an ICEV (Kia Rio 1.0 T-GDI 120, 2019) and an EV (Kia e-Niro, 150 kW, 2019), in which the AVAS was either activated or deactivated. The recordings were collected while driving with well-defined velocity profiles (various constant speeds, various conditions with acceleration). We recorded the vehicle sound with four free-field microphones mounted at different positions on the chassis. During the acoustic recordings, the trajectory of the vehicle was measured with highly precise GPS position

tracking. In the auditory VR simulations, the microphone signals recorded on the test track are then used as sound sources in an acoustic VR simulation software (TASCAR; Grimm et al., 2019) and are animated on the basis of the GPS position tracking data. Using this approach, it is possible to present real vehicle sounds, and to simulate the exact vehicle motion during the vehicle recordings. Further details regarding the acoustic recordings of the vehicle sounds are described in a previous article by Oberfeld et al. (under review). The interactive auditory VR simulations can be combined with interactive three-dimensional visual VR simulations presented stereoscopically on a head-mounted display.

Auditory VR simulation and sound reproduction

A physically plausible interactive simulation of the dynamic spatial sound field corresponding to an urban traffic scene with an approaching vehicle was realized with the auditory VR software TASCAR (Grimm et al., 2019). TASCAR offers dynamic processing of the geometry of the acoustic scene (time-variable positions of (image) sound sources, absorbers and receivers), acoustic modeling of the sound transmission from the sources to the receiver, and sound field synthesis. TASCAR models the directional characteristic of sound sources, the distance-dependent change of the sound level caused by spherical spreading and air absorption, and the distance-dependent sound travel time (which can lead to, e.g., Doppler effects). Sound reflections on the ground and other surfaces are simulated by the image sound source method (Allen & Berkley, 1979), so that, for instance, time-variant comb-filter effects due to acoustical interference between reflected and direct sound are simulated. Due to the higher-order Ambisonics rendering (see below), dynamic changes in the interaural level and time differences resulting from changes of the position of the sound sources relative to the head of the listeners are also simulated, and the listeners can interact with the acoustic scene, i.e., listen around with head movements. In the present experiment, the processing of the dynamic geometry of the acoustic scene was based on the GPS position data acquired during the acoustic recordings on the test track. Thus, the motion of the cars presented in the simulations was identical to the motion of the real cars on the test track. The simulated ear height of the receiver matched the actual ear height of each listener in an upright position.

A spatial sound field was generated using sound field synthesis, namely 2D 7th-order Ambisonics (Ahrens et al., 2014; Zotter & Frank, 2019). The Ambisonics approach assumes sound reproduction in an acoustic free field. When preparing the laboratory space, special attention was therefore paid to reducing acoustic reflections. The rectangular laboratory area containing the speaker array (dimensions: 570 cm × 450 cm) was separated from the larger lab space (105 m^2) with sound-absorbing acoustic curtains (Gerriets Bühnenvelours Ascona 570; 570g/m^2; absorption coefficient of 0.95 for frequencies above 400 Hz). The parts of walls and ceiling adjacent to the speakers were lined with Basotect acoustic foam panels (BASF; 10 cm thickness, absorption coefficient of at least $\alpha = 0.9$ at frequencies above 400 Hz).

Within the rectangular laboratory area, a circular array of 16 loudspeakers (Genelec 8020DPM-7) was installed. The radius was 2.0 m, the minimum distance of the loudspeakers to the walls was about 40 cm, and the minimum distance to the acoustic curtain was about 20 cm. The loudspeakers were positioned at an equal angular distance of 22.5°. The tweeters of the two-way speakers were located 160 cm above the floor and thus close to the average upright ear height of adults (Gordon et al., 1989). The floor within the loudspeaker array was covered with a thick carpet (IKEA Stoense), which also covered the loudspeaker bases. The monitors and computers used for the experiment were located adjacent to the loudspeaker array and were also shielded with acoustic foam panels.

The simulated auditory traffic scene was presented using the Ambisonics loudspeaker array. The 16 loudspeakers of the array were controlled by an audio converter (Ferrofish Pulse 16, 24 bit audio resolution, f_s = 44.1 kHz), which received the audio signals from an RME HDSPe RayDAT audio card in the computer running TASCAR. Acoustic calibration of the loudspeaker array was performed using the TASCAR Speaker Calibration Tool and a sound level meter (Norsonic Nor131

with Roga MP40 free field microphone) placed in the center of the loudspeaker array and 165 cm above the floor. During calibration, level differences between the 16 loudspeakers were compensated and the sound pressure levels of a point source and a diffuse sound field were calibrated. The sound levels from the calibrated microphones mounted on the vehicles during the recordings on the test track were used to set the sound levels of the simulated sound sources.

Visual VR simulation

The interactive auditory VR simulation was combined with visual VR simulations of the traffic scenes. The participants viewed the visual traffic scene stereoscopically wearing a head-mounted display (HTC Vive Pro; 1440 × 1600 pixels per eye, 90 Hz frame refresh rate, 110° field of view). Laser-based head and motion tracking of the head-mounted display enabled the transformation of real head movements into virtual head movements, thus allowing participants to explore the visual scene. The height of the virtual camera above the simulated floor corresponded to the real eye level of the participant, as recorded by the head tracking. The simulations were created using the VR-software WorldViz Vizard 5.0 on a Windows computer (Intel Core i9-9900X CPU @ 3.50 GHz, Nvidia Quadro RTX 4000). The Vizard script also sent commands controlling the corresponding acoustic simulations in TASCAR via the OSC network protocol (http://opensoundcontrol.org/), so that the auditory and visual VR simulations were synchronized in time.

Stimuli and procedure

Audiovisual simulated traffic scenes

In the experiment, audiovisual virtual traffic scenes were presented in which a vehicle approached the participant's position on a straight trajectory on the right lane of a two-lane road (see Figure 1). The vehicle either travelled at constant speed for 5.0 s, or travelled at constant speed for 2 s before accelerating for 3 s. Participants experienced the virtual scene from a pedestrian's perspective. Their position in the virtual scene was 50 cm away from the right curb, typical for a pedestrian intending to cross the street.

The visual virtual road scene was modelled after the Eislebener Straße in Berlin, using 3DS Max 2020.2 and 3D data provided by the Senate Department for Urban Development and Housing of the City of Berlin (https://www.stadtentwicklung.berlin.de/planen/stadtmodelle/de/digitale_innenstadt/3d/index.shtml). The 3D model of it depicted an urban two-lane road (length approx. 300 m, width 6.5 m, lane width 3.25 m) without bends or curves as well as a uniform, gapless front of houses at the roadside (see Figure 1). The distance between the house fronts on the right side of the street and the right lane marker was 8.4 m. The distance between the house fronts on the left side of the street and the right lane marker was 15.6 m. Unlike in the original street, the virtual street scene did not include any vehicles, bicycles, signs, etc. White road markings were added as well as a blue line reaching from one side of the road to the other. The blue line was placed at a distance of 50 cm to the left of the participant's position in the virtual scene and served for orientation in the virtual environment. The approaching car was modelled after a red Mitsubishi Colt (L × W × H = 3.810 m × 1.895 m × 1.520 m). A male avatar with a neutral facial expression was presented on the driver's seat. The same visual car model was presented on all trials. It thus did not differ between the vehicle types (ICEV, EV, EV+AVAS).

In the simulated acoustic scene, the geometry of the ground surface and the house fronts was identical to the visual scene. The surfaces were simulated with plausible acoustic reflection properties. Based on (ISO 9613-2:1999-10, 1999), the reflectance of the ground surface was set to $\rho = I_r/I_0 = 1.0$, where I_r is the acoustic intensity of the reflected sound wave and I_0 is the intensity of the incoming wave. Thus, we modeled both the road surface and the adjacent ground surface areas as acoustically hard. Based on the same standard, the reflectance of the house fronts was set to $\rho = 0.8$. The sound reflections were modeled with an IIR low pass filter of first order with a

cut-off frequency of 5 kHz. The parameter *scattering* in TASCAR describes random deviations in the sound reflection and was set to a value of 0.5. A first-order Ambisonics recording from a quiet residential area was presented as background noise (L_{Aeq} = 37.5 dB).

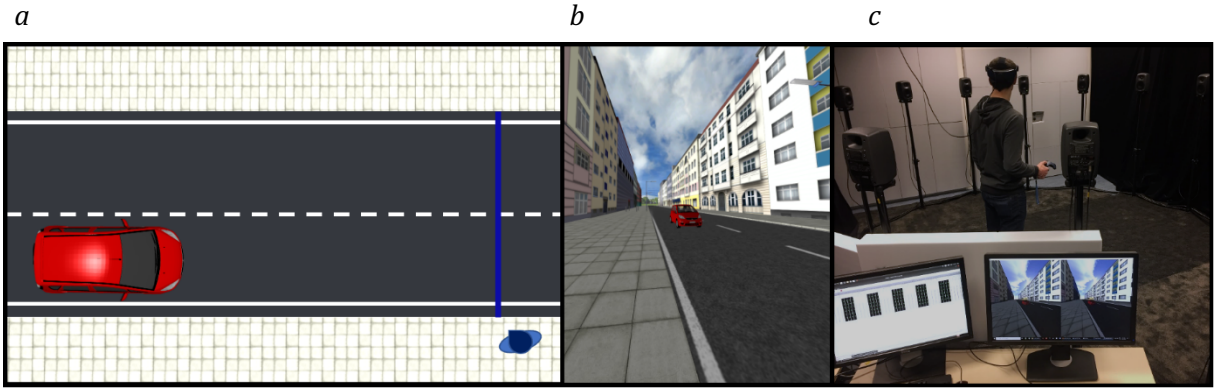

Figure 1 — a) Bird's-eye view of the simulated street scene, b) the participants' view of the street scene, and c) a participant in the loudspeaker array wearing the head-mounted display and holding the controller. The vehicle drove along the street towards the virtual position of the participants, which was marked with a blue line for reference. The participants observed and listened to the vehicle approach and estimated its TTC.

Time-to-collision (TTC) estimation: Prediction-motion task

TTC estimates were obtained in a prediction-motion task (Schiff & Detwiler, 1979), which is one of the tasks most frequently used in the literature to study TTC estimation. Participants wore the head-mounted display, stood in the center of the loudspeaker array and experienced the simulated audiovisual traffic scene described above (Figure 1). Their position in the virtual scene was 50 cm away from the right curb. When they turned their heads to the left side, they were able to see the vehicle along the street. They were instructed to press a button on the controller to start the vehicle's motion. Independent of the driving profile, the vehicle was visible and audible for 5.0 s before it was "occluded", that is, it was then no longer audible and visible. The temporal and spatial distance of the vehicle at occlusion was defined by the different simulated TTCs, accelerations and velocities (see the following paragraph). Participants were instructed to pull the trigger of the controller when they thought that the approaching vehicle would have reached the blue line on the street, if the vehicle had continued to approach them after occlusion at the same constant speed or acceleration as observed before occlusion. The time interval between the occlusion and the manual response was taken as the participant's estimate of the TTC of the vehicle at the moment of occlusion.

Experimental conditions

The ICEV and EV with and without AVAS either continuously approached the participant at a constant velocity (a = 0 m/s^2), or accelerated (a > 0 m/s^2) after initially travelling at a constant velocity. During the constant-velocity approaches, the nominal velocity v_0 was 10, 20, 30, 40, and 50 km/h. During the accelerated approaches, the initial constant velocity (before the onset of acceleration) and the acceleration level were varied. The nominal initial velocity v_0 was 10, 20, 30, and 40 km/h, whereas the nominal acceleration level a was 0.6 and 2 m/s^2, respectively. Since the AVAS was active at velocities up to 28 km/h, the EV with AVAS was only represented in respective driving conditions. Table I shows the presented 31 combinations of driving profile and the three vehicle types (ICEV, EV, EV+AVAS), and indicates the number of available acoustic recordings per combination. Note that the presented driving profiles did not exactly match the nominal driving profiles because the stimuli were based on real drives on a test track, as described in more detail below.

Table I — Presented nominal driving conditions for each of the vehicle types (ICEV = internal combustion engine vehicle, EV = electric vehicle without AVAS, EV+AVAS = electric vehicle with AVAS). The cells indicate the number of available acoustic recordings in the respective combination of driving profile and vehicle type. For the ICEV, the number in brackets shows how many acoustic recordings included a manual gear shift.

Driving conditions		**Vehicle type**		
a **[m/s²]**	v_0 **[km/h]**	**ICEV**	**EV**	**EV+AVAS**
0.0	10	3 (0)	2	2
0.0	20	2 (0)	3	3
0.0	30	1 (0)	4	
0.0	40	2 (0)	2	
0.0	50	2 (0)	1	
0.6	10	3 (2)	3	3
0.6	20	3 (0)	1	1
0.6	30	6 (0)	2	
0.6	40	3 (0)	2	
2.0	10	3 (3)	3	4
2.0	20	6 (0)	3	
2.0	30	3 (0)	2	
2.0	40	1 (0)	1	

The 31 combinations of velocity, acceleration level and vehicle type were all paired with three actual TTCs (2.0, 3.5, and 5.0 s), which resulted in 93 experimental conditions. The actual TTC was defined as the time interval between occlusion and the time at which the vehicle would have arrived at the participants' location if it had continued its motion in the same manner as during the presentation (i.e., at the same constant velocity or acceleration before occlusion). Based on an average walking speed of a pedestrian of 1.44 m/s (Ishaque & Noland, 2008), it would take 2.26 s to cross the 3.25 m wide right lane of the simulated road. Based on this assumption, the initiation of a road-crossing at a TTC of 2.0 s would result in a collision between the pedestrian and the vehicle in the real world. At a TTC of 3.5 s, the pedestrian would be able to cross the right lane where the vehicle is approaching without collision. At a TTC of 5.0 s, the pedestrian would be able to safely cross both lanes before the vehicle arrives at her or his position.

For each acoustic recording that represented a combination of acceleration, velocity and vehicle type, the three different TTCs were generated by shifting the distance of the vehicle at occlusion in the audiovisual simulation. For constant-velocity approaches, we used the equation of motion $D(TTC) = v \cdot TTC$, where *D(TTC)* is the distance between the vehicle's front and the participant's position along the road at the time of occlusion for a desired TTC and the vehicle's constant velocity v. Since the recorded drives at constant velocities mostly showed small deviations from the intended velocity, the average velocity v_{avg} across the presentation duration, computed from the GPS data of the respective acoustic recording, was used in the equation.

To generate the desired TTCs for the accelerated vehicle approaches, the velocity at occlusion onset (v_{occ}) was determined from the GPS data for each recording. In addition, the average acceleration a_{avg} was calculated within a time window of 1.0 s before occlusion onset. Using v_{occ} and a_{avg}, the distance of the vehicle at occlusion corresponding to the desired TTC at occlusion was set to $D(TTC) = \frac{1}{2}(a_{avg} \cdot TTC^2 + 2TTC \cdot v_{occ})$.

Each of the 93 experimental conditions was presented once in each of seven experimental blocks. Thus, each participant judged the TTC for each experimental condition seven times, resulting in 651 experimental trials per participant. The order of the experimental conditions within each block was randomized. We took into account that there was usually more than one acoustic recording available per experimental condition (Table I). All of them were presented in order to increase the ecological validity. For this purpose, an iterative procedure was used to generate a sequence of seven acoustic recordings per experimental condition, which was randomly generated, but in such a way that each recording available for the corresponding condition was included at least once. Each acoustic recording from this sequence was then presented in exactly

one of the seven experimental blocks. For each trial with a constant-velocity approach, we additionally selected a random time interval of 5.0 s from the available recording duration. Thus, the sound of the same acoustic recording of a constant-velocity approach could differ slightly from presentation to presentation, again increasing the ecological validity. The seven experimental blocks were divided into four sessions, with only one block presented in the first session and two blocks presented in each of the remaining sessions.

Comparison of driving profiles between the vehicle types

Since many of the driving profiles recorded on the test track deviated slightly from the intended nominal driving profiles due to the technical challenges, these deviations were first compared between the vehicle types in order to be able to adjust the subsequent data analysis accordingly. A preliminary analysis of the data showed that one of the presented constant velocity drives (EV at v_0 = 20 km/h) had an acceleration of −0.4 m/s² in the presented time window. Trials that included this acoustic recording were excluded from further analysis. This affected only 21 of the total 19530 trials collected in the experiment.

For constant-velocity approaches, the mean velocity presented v_{avg} was similar for all intended nominal velocities v_0 and similar for all three vehicle types, except for one recording (ICEV v_0 = 50 km/h). The mean constant velocities driven differed between the vehicle types at all intended nominal velocities by a maximum of 2.3 km/h on average.

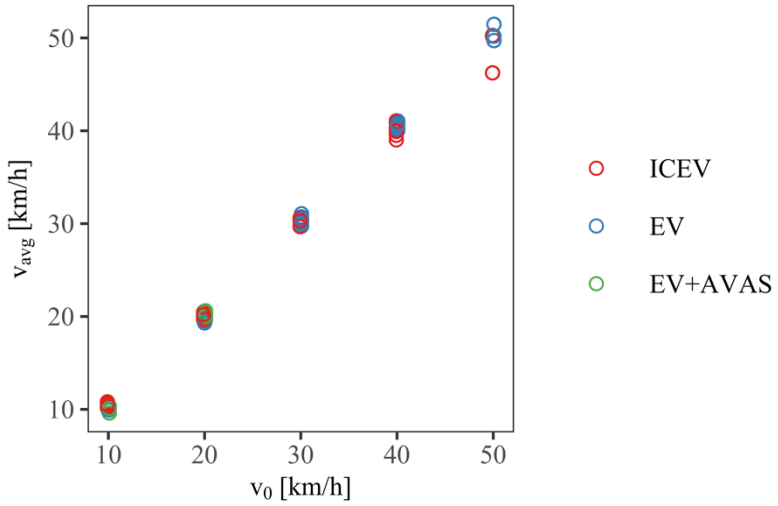

Figure 2 — Mean presented constant velocity v_{avg} (y-axis) as a function of the intended nominal velocity v_0 (x-axis) for each of the presented acoustic recordings of constant velocity drives. The colors indicate the vehicle type: red = ICEV, blue = EV without AVAS, green = EV with AVAS.

For accelerated vehicle approaches, Figure 3 shows the presented velocity at occlusion (v_{occ}) and the mean acceleration presented within the last second before occlusion (a_{avg}) for the three vehicle types. These recorded drives show deviations between the nominal and actual acceleration, as well as a variation in velocity at occlusion. However, at an intended acceleration a = 0.6 m/s² (left panel), the v_{occ} and a_{avg} presented in the experiment varied in a comparable range for all three vehicle types. At an intended acceleration of a = 2.0 m/s² and initial velocities higher than v_0 > 10 km/h (and accordingly higher v_{occ}), however, a_{avg} tended to be higher for the ICEV than for the EV without AVAS. At an intended initial velocity v_0 = 10 km/h, on the other hand, a_{avg} for the ICEV tended to be below the values for the two EVs.

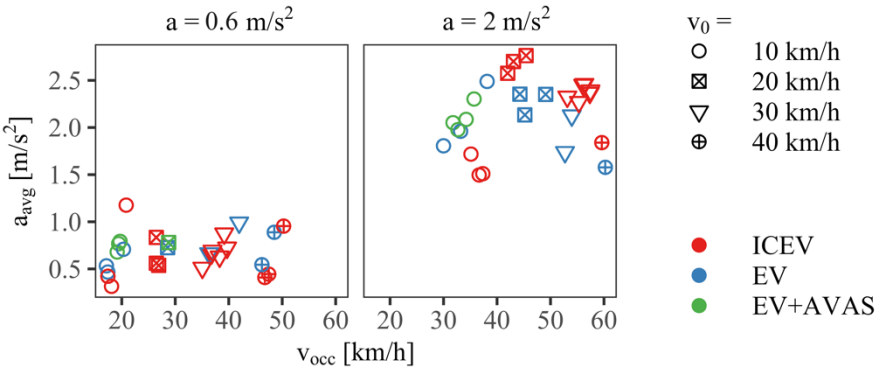

Figure 3 — Mean acceleration within the last second before occlusion a_{avg} (y-axis) as a function of the velocity at occlusion v_{occ} (x-axis) for each of the presented acoustic recordings. The panels represent the nominal acceleration level a: left = 0.6 m/s², right = 2.0 m/s². The shapes indicate the nominal initial velocity v_0: circles = 10 km/h, crossed squares = 20 km/h, triangle = 30 km/h, crossed circles = 40 km/h. The colors indicate the vehicle type: red = ICEV, blue = EV without AVAS, green = EV with AVAS.

From a driving perspective, some of the differences between the accelerating ICEV and EV could be related to gear shifts in the ICEV. For example, at an intended initial speed of v_0 = 10 km/h and an intended acceleration of a = 0.6 m/s², two of the three acoustic recordings available for the ICEV included a gear shift (Table I). At an intended initial speed of v_0 = 10 km/h but an intended acceleration of a = 2.0 m/s², all recordings of the ICEV contained a gear shift.

To account for the variation in the actual velocities and accelerations and thus to avoid confounding the effect of vehicle type by differences in presented accelerations, the data analysis for the accelerated vehicle approaches did not use the intended nominal velocities and accelerations as independent variables. Instead, regression analyses were used that included the actually presented velocities and accelerations of each acoustic recording as continuous predictors. This ensured that statistical differences in the TTC estimations between vehicle types could not be attributed to confounding influences of the variation in driving profiles between the vehicle approaches. The resulting statistical model of the data can also be used to predict TTC estimates in combinations of initial speed and acceleration that were neither recorded nor presented in the experiment.

Experimental sessions

The experiment consisted of four sessions. In the first session, participants received information about the upcoming experiment, gave written informed consent and completed demographical questions, vision and hearing tests. The experimenters additionally measured the participant's ear height and inter-pupillary distance. The individual ear height was used to adjust the height of the simulated receiver above the ground surface accordingly. The individual inter-pupillary distance was used to set the distance between the two displays of the head-mounted display. To detect potential motion-sickness symptoms during the experiment, the participants rated their motion-sickness on the Fast Motion-Sickness Scale ranging from 0 ("no sickness at all") to 20 ("frank sickness") (Keshavarz & Hecht, 2011) prior to testing as baseline, and after each experimental block. No issues with motion sickness occurred. Subsequently, they received instructions for the upcoming prediction-motion task. To get familiar with the simulated traffic scene and the task, participants completed a training block with 31 trials, which were later excluded from the analyses. Subsequently, participants completed the first experimental block. Participants were given the opportunity to take a break anytime during the experiment, but after half of the trials (after approximately 20 minutes) of each session, the participants were asked to take a break and rest. In each of the remaining three sessions, two experimental blocks of the prediction-motion task were presented. At the beginning of each of these sessions, there were

five training trials. After completing all experimental blocks, participants completed a final questionnaire regarding their personal experience with EVs, driving experience, and experience of the experiment. The experiment lasted approximately 4.5 to 5 hours.

Participants

Thirty participants with (corrected-to-)normal vision and normal hearing(25 female, 5 male; M = 26.37 years, SD = 8.87 years) completed the experiment. Visual acuity, stereoscopic acuity and hearing thresholds were assessed prior to testing. Audiometric hearing thresholds were measured bilaterally using Békésy audiometry with pulsed 270 ms pure tones. The hearing thresholds on both ears of all participants were measured in a frequency spectrum between 125 Hz and 4000 Hz and did not exceed 20 dB HL. Landolt's C test of the Freiburg Visual Acuity Test (Bach, 1996) was used to test for the required visual acuity of at least 1.0. The stereoscopic acuity was tested with a Titmus Test (A. G. Bennett & Rabbetts, 1998), presented on the head-mounted display. Correction of visual acuity was possible with contact lenses but not with glasses, because the latter limited the optimal fit of the head-mounted display. Participants with a seizure disorder were not allowed to take part in the experiment, since the use of electronic displays can cause the occurrence of a seizure. The participants were not informed about the experimental hypotheses

The experiment was conducted in accordance with the ethical principles of the Helsinki Declaration and the Ethics Committee of the Institute of Psychology of the Johannes Gutenberg University Mainz (approval number: 2019-JGU-psychEK-S011). All participants volunteered for course credit or monetary reward (7 € per hour). Prior to testing, but after study information was provided and possible risks were explained, they gave their written consent.

The sample size was chosen so that, in the repeated-measures design used here, differences in behavioral measures (e.g., mean TTC estimate) between two given conditions (e.g., ICEV vs. EV) could be detected at a relatively small effect size in the population, d_z = 0.53 (Cohen, 1988), with a test power of 80% (α = .05).

Results

Statistical analyses of the TTC estimates for accelerating vehicles

Since the AVAS was only active for velocities up to 28 km/h, we analyzed the TTC estimates for accelerating vehicles in two parts. In the first part, we analyzed the TTC estimates for the ICEV and EV without AVAS because these vehicle types were presented in a larger range of driving profiles. In the second part, we focused on the two lowest initial velocities ($v_0 \leq 20$ km/h) where all three vehicle types (ICEV, EV, EV+AVAS) were presented. For the illustration of the observed TTC estimates, we used outlier-corrected data. For each combination of participant, acoustic recording and TTC, the collected TTC estimates were examined for outliers using the Tukey method (Tukey, 1977), if at least five trials were available in a given combination. Data points that were more than three interquartile ranges below the first or above the third quartile were excluded from the figures as outliers. For the statistical analysis of the TTC estimates for accelerating vehicles via linear mixed-effects models (LMMs), we used regression diagnostics to detect outlying or influential data points (see below). The LMMs with random intercepts accounted for the actually presented accelerations a_{avg}, which differed from the intended nominal accelerations a, and the actually presented velocities at occlusion v_{occ}. They contained a_{avg} and v_{occ} as continuous predictors.

In the context studied here, it is primarily relevant to make predictions for other, future traffic situations from the data collected in the experiment. With respect to the bias-variance tradeoff in statistical analyses (see, e.g., James et al., 2013), we considered it more important to formulate a robust statistical model with a low prediction error than to fit a model that represents the

available data as accurately as possible (Yarkoni & Westfall, 2017). Therefore, we used a cross-validation approach to select the variables to be included as predictors in the regression models. The 10-fold cross-validation is a procedure in which the data set is first randomly divided into 10 parts. In each iteration, 9 of the 10 parts are used as the training set to which the statistical model is fitted. The remaining 10th part is used as the test set. The regression model is fitted to the training data set and is then applied to the test set. For each data point in the test set, the prediction error is registered as the squared deviation of the predicted value from the observed value (estimated TTC). Thus, the predictive accuracy of the model is tested for data that did not enter into the estimation of the model parameters. This procedure is performed for each of the 10 possible splits in training and test set. To further increase statistical robustness, the cross-validation was performed twice for each possible regression model. The sum of squared prediction errors (predicted residual sum of squares; PRESS) was used as the goodness-of-fit measure in the model selection.

TTC estimates for accelerating ICEVs and EVs

For the statistical analysis of the TTC estimates for the accelerating ICEV and EV without AVAS (first regression model), the model selection considered all of the 32767 possible combinations of the four predictors vehicle type, actual TTC, v_{occ}, and a_{avg} (main effects and interaction effects). For each of the 32767 models variants, the cross-validation procedure determined the PRESS of an LMM with random intercept (R function lmer()). Of these models, 16 models showed the lowest, identical prediction error (PRESS = 1805.20). The model selected from the 16 models was the one that was most parsimonious, i.e., the one that could describe the estimated TTC (TTC_{est}) with the lowest number of model terms. The model equation of the selected regression model was:

$$\mathrm{TTC_{est}} \sim \mathrm{TTC} + \mathrm{TTC} \times v_{\mathrm{occ}} + \text{vehicle type} \times v_{\mathrm{occ}} + \text{vehicle type} \times \mathrm{TTC} \times a_{avg} + \text{vehicle type} \times a_{avg} \times v_{\mathrm{occ}} + \text{vehicle type} \times \mathrm{TTC} \times a_{avg} \times v_{\mathrm{occ}}$$

The selected regression model was fitted to the trials presenting the accelerating ICEV and EV without AVAS. The categorical predictor *vehicle type* was dummy coded. Variance components were estimated using the restricted maximum likelihood (REML) method. For the statistical tests, the Kenward-Roger approximation of the degrees of freedom was used (Kenward & Roger, 1997). 117 trials for which the absolute value of the externally studentized residual was greater than 4.0 or for which the index DFFITS (Belsey et al., 2005) was more than five interquartile ranges below the first quartile or above the third quartile were categorized as outliers, and excluded from the analysis. A total of 9963 trials were included in the analysis of the accelerating ICEV and EV without AVAS. The model explained 71.20% of the variance in the data with its random and fixed effects. The variance explained by the fixed effects was $R^2_{marginal}$ = 0.43 (Nakagawa & Schielzeth, 2013).

Figure 4 shows the mean TTC estimates as a function of actual acceleration presented. The horizontal dashed line represents the actual TTC and corresponds to a perfect TTC estimation. Data points above the horizontal dashed line correspond to an overestimation of TTC. Such an overestimation of TTC poses a potential risk in a road-crossing situation, as participants assume that the vehicle would arrive later at their position than it actually does, and therefore decide to cross before an approaching vehicle even though the time remaining is too short. In contrast, data points below the horizontal dashed line represent an underestimation of TTC. Although the underestimation of TTC corresponds to an estimation error, it does not pose a direct risk in a road-crossing situation.

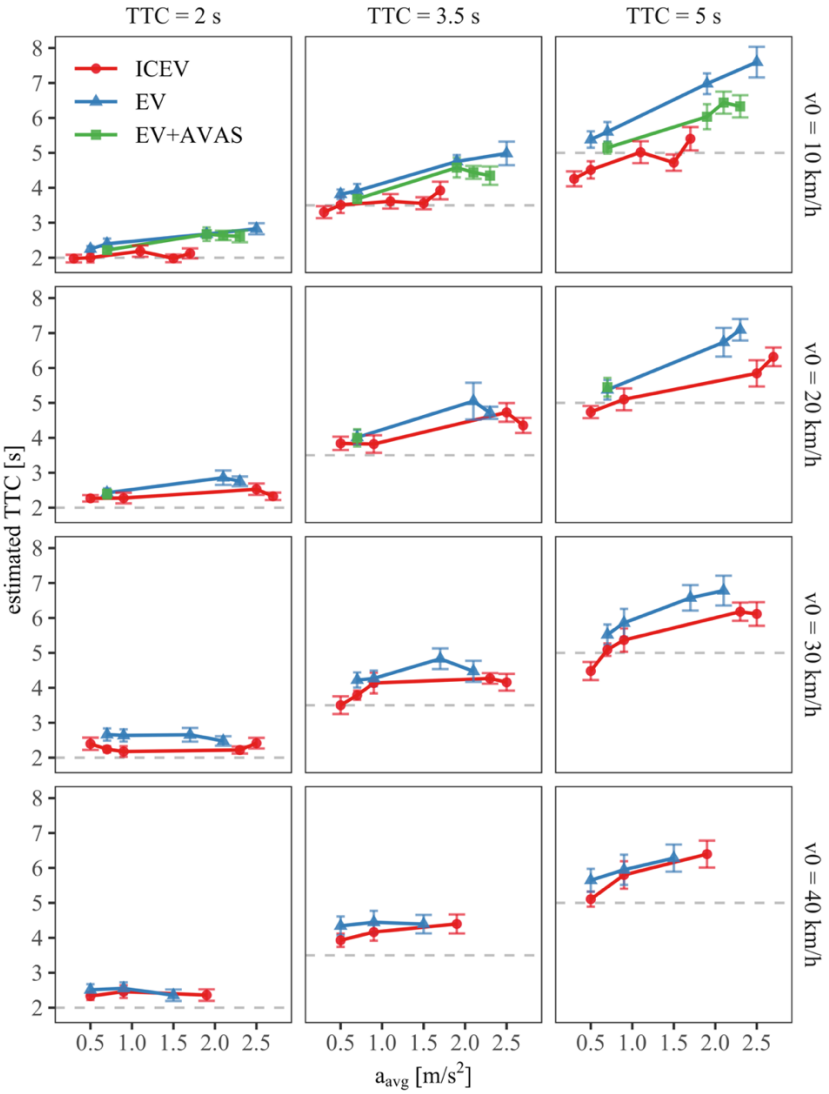

Figure 4 — Mean TTC estimates for accelerating vehicles (y-axis) as a function of the acceleration within the last second before occlusion a_{avg} (x-axis). Each row represents a nominal initial velocity v_o, each column indicates a presented actual TTC. The panels represent the intended nominal acceleration level a: left = 0.6 m/s^2, right = 2.0 m/s^2. The colors indicate the vehicle type: red = ICEV, blue = EV without AVAS, green = EV with AVAS. The gray dashed line represents a perfect estimate of the TTC. Error bars represent ± 1 SE of the mean. Bin width = 0.2 m/s^2.

As expected from the literature, the TTCs were systematically overestimated for the accelerating vehicles. On average, the overestimation of TTC also increased with increasing acceleration a_{avg} and with increasing actual TTCs. This pattern is similar to a first-order estimation indicating that participants did not adequately account for the vehicle's acceleration in their TTC estimates (e.g., Benguigui et al., 2003). If participants adequately considered the acceleration, the estimated TTC would not increase as a function of acceleration or actual TTC. Across the different initial velocities, accelerations, and actual TTCs, the overestimation of TTC was on average more pronounced for the EV with and without AVAS than for the ICEV. The TTC estimates for the accelerating EV with and without AVAS increased more strongly as a function of acceleration and actual TTC than for the ICEV. This pattern of first-order estimation is consistent with our hypothesis that the acceleration is less well accounted for in TTC estimation for the electric vehicles. Nonetheless, the first-order pattern was slightly less pronounced for the EV with AVAS compared to the EV without AVAS, indicating that the AVAS partially promoted the consideration

of acceleration during TTC estimation. Because the difference between a first- and second order estimation decreases with increasing velocity, it is not surprising that the effect of vehicle type was most pronounced at the lowest initial velocity (v_0 = 10 km/h). At higher initial velocities, in contrast, the estimated TTCs for the ICEV and EV without AVAS were more similar on average. For instance, at v_0 = 40 km/h and an actual TTC = 5.0 s (bottom right panel), the TTCs estimated for the ICEV and EV similarly increased with increasing acceleration. That is, under these conditions, a similar first-order pattern was observed for the ICEV as for the EV without AVAS. This could be associated with the fact that the powertrain noise of the ICEV, which helped estimating the TTC in a lower velocity range, was now dominated by other noises, such as the tire or aerodynamic noises.

The estimated fixed effects parameters of the model predicting the TTC estimates for the accelerating ICEV and the EV without AVAS are given in Table II. Of particular relevance here are the interaction effects between acceleration a_{avg}, vehicle type, and velocity at occlusion v_{occ}. The estimated TTC of the EV increased more strongly as a product of actual TTC and acceleration (EV × TTC × a_{avg}: β = 0.3074) than for the ICEV (ICEV × TTC × a_{avg}: β = 0.0413), $F(2,9933) = 128.49$, $p < .001$. In addition, when the velocity at occlusion was high, the estimated TTC increased less strongly as a function of acceleration for both vehicle types (ICEV × v_{occ} × a_{avg}: β = -0.0055, EV × v_{occ} × a_{avg}: β = -0.0077), although the decrease in the effect of acceleration with increasing v_{occ} was still significantly smaller for the ICEV than for the EV without AVAS, $F(2,9933) = 14.12$, $p < .001$. Since high velocities at occlusion occurred primarily at high initial speeds, this replicates the pattern observed in Figure 4, where the difference between the TTC estimates for the ICEV and EV was maximal at the lowest initial speed. These interactions are compatible with the hypothesis that the acceleration of the EV without AVAS was less well accounted for in the TTC estimation (first-order estimation) than the ICEV's acceleration, especially in a lower velocity range.

Table II — Estimated fixed effects parameters of the model predicting the TTCs estimates for the accelerating ICEV (internal combustion engine vehicle) and EV (electric vehicle without AVAS). Given are effect estimates (β), standard errors (*SE*), degrees of freedom (*df*), *t*-, and *p*-values.

	β	*SE*	*df*	*t*	*p*
(Intercept)	0.4921	0.2344	58	2.13	.037
TTC	0.7223	0.0379	9933	19.07	< .001
ICEV × v_{occ}	0.0026	0.0041	9933	0.62	.535
EV × v_{occ}	0.0067	0.0041	9933	1.62	.105
TTC × v_{occ}	0.0036	0.0012	9933	2.99	.003
ICEV × TTC × a_{avg}	0.0413	0.0208	9933	1.99	.047
EV × TTC × a_{avg}	0.3074	0.0218	9933	14.12	< .001
ICEV × v_{occ} × a_{avg}	-0.0055	0.0013	9933	-4.23	< .001
EV × v_{occ} × a_{avg}	-0.0077	0.0015	9933	-5.19	< .001
ICEV × TTC × v_{occ} × a_{avg}	0.0017	0.0006	9933	3.07	.002
EV × TTC × v_{occ} × a_{avg}	-0.0024	0.0006	9933	-3.88	< .001

The selected regression model can now be used to predict the effect of acceleration (a_{avg}), vehicle type, actual TTC, and velocity at occlusion (v_{occ}) on the TTC estimates. This model prediction represents the expected pattern, correcting for the "noise" in the collected data. In addition, predictions can be made for combinations of a_{avg} and v_{occ} beyond those presented in the experiment. Figure 5 shows the predicted TTC estimates for accelerating vehicle approaches as a function of a_{avg}, vehicle types, v_{occ}, and actual TTC. The gray dashed line represents a perfect TTC estimation. The yellow dashed line represents a first-order TTC estimate where the acceleration is not considered (Benguigui et al., 2003). The first-order estimate is defined as follows, $TTC1 = \frac{D_{occ}}{v_{occ}} = TTC + \frac{a_{avg} \cdot TTC^2}{2 \cdot v_{occ}}$, where D_{occ} denotes the distance between the vehicle and the participant at occlusion and TTC denotes the actual TTC (considering the acceleration). From the equation and the dashed orange lines in Figure 5, it can be seen that the overestimation of TTC for a first-order estimation increases with a_{avg} and actual TTC and decreases with v_{occ}. The pattern of TTC estimates predicted by the model is, of course, similar to the pattern of the measured TTC estimates on which the model is based (Figure 4). The predicted TTC estimates show that as a_{avg} increases, increasing overestimation of TTC can be expected. This effect of acceleration is more pronounced at longer actual TTCs and lower v_{occ}, and thus the predicted TTC estimates show a pattern similar to a first-order estimation. The new and important finding in the present data is that this first-order pattern is much more pronounced for an EV without AVAS than for an ICEV. Even with the longest TTC of 5.0 s and the two lowest v_{occ} *values*, the predicted estimated TTCs for the ICEV are quite similar to the veridical TTC values. For the EV, in contrast, the model predicts a strong linear increase in TTC estimates with a_{avg}, resulting in an overestimation of TTC by more than one second at an acceleration of 2.0 m/s^2. The pattern is compatible with our hypothesis that the altered acoustic signature of the EV without AVAS results in problems in accounting for the acceleration during TTC estimation.

At the highest v_{occ} analyzed in Figure 5, the predicted TTC estimates for the EV are similar to those for the ICEV and the influence of acceleration on the TTC estimates for the EV is significantly reduced. A plausible explanation for this finding is that the difference between the first-order estimate and the actual TTC decreases as v_{occ} increases. Thus, the error in the TTC estimate that would result from a first-order TTC estimation for the EV without AVAS is reduced, as depicted by the orange (first-order TTC estimates) and gray (actual TTCs) dashed lines in the plots.

Taken together, the descriptive data and the predictions of the regression model fitted to the data clearly showed a less pronounced first-order pattern for the accelerating ICEV than for the accelerating EV without AVAS. In some cases, participants estimated the TTC for accelerating EVs to be significantly longer than it actually was, potentially creating risky situations in real-world traffic. The predicted overestimation of TTC occurs mainly for the strongly accelerating EV in the low velocity range and for a long actual TTC. However, even across accelerations, velocities, and actual TTCs, the predicted overestimation of TTC is more pronounced on average for EVs than for ICEVs. At each acceleration level, the predicted TTC estimates for the EV without AVAS exceed the predicted TTC estimates for the ICEV except at the highest v_{occ} (Figure 5).

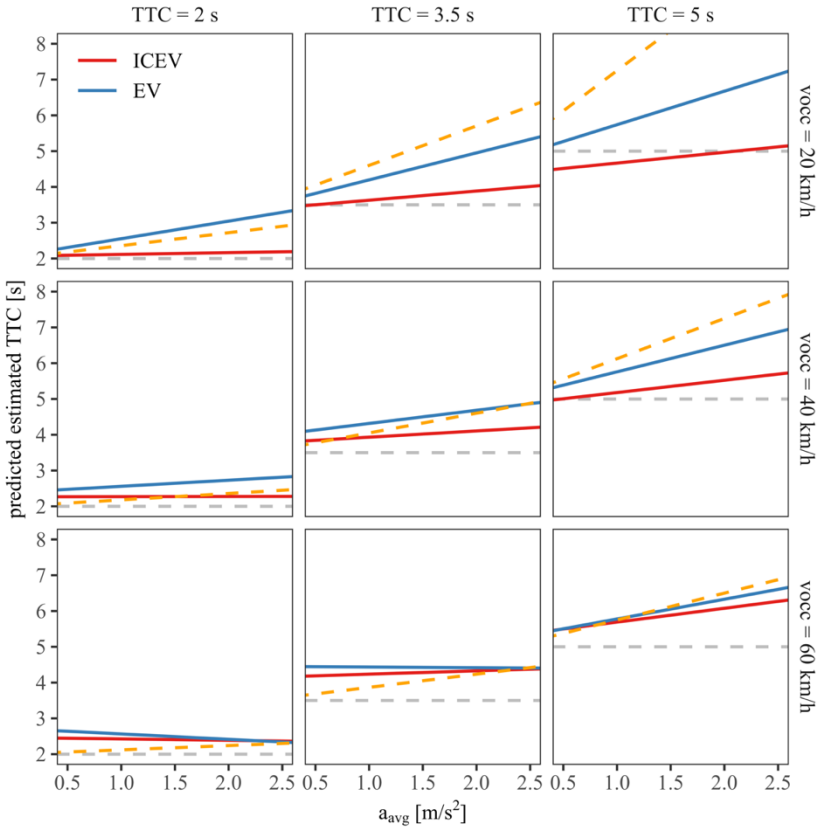

Figure 5 — TTC estimates predicted by the regression model for accelerating ICEV and EV without AVAS (y-axis) as a function of acceleration (x-axis), vehicles types (color coding), velocity at occlusion (rows), and actual TTC (columns). The gray dashed line represents a perfect estimate of the TTC. The yellow dashed line represents the first-order TTC estimate. Color coding: red = ICEV, blue = EV without AVAS.

TTC estimates for accelerating ICEVs, EVs with and without AVAS at v_0 = 10 km/h

At v_0 =10 km/h, all three vehicle types (ICEV, EV, EV+AVAS) were presented in the experiment at the nominal acceleration level a = 0.6 m/s² and 2.0 m/s². The same analysis approach as used in the previously described analysis was used. The most robust regression model was again selected by cross-validation. Here, four models had the lowest, identical prediction error (PRESS = 611.93), of which the most parsimonious model was selected to analyze the accelerated vehicle approaches at v_0 = 10 km/h. The model equation was:

$$TTC_{est} \sim TTC + \text{vehicle type} \times a_{avg} + TTC \times a_{avg} + \text{vehicle type} \times TTC \times v_{occ}$$

The same regression diagnostics as above were used to exclude outliers from the analysis (0.66% of the 3780 trials). A total of 3755 trials were included in the analysis of the accelerating ICEV, EV and EV with AVAS. The model explained 69.81% of the variance in the data with its random and fixed effects. The variance explained by the fixed effects was $R^2_{marginal}$ = 0.47.

Table III shows the estimated fixed effects parameters of the model predicting the TTC estimates for the accelerating ICEV, EV with and without AVAS at an initial velocity of 10 km/h, and Figure 6 shows the corresponding predicted TTC estimates. For the prediction, v_{occ} was set to 26.69 km/h, which is the average v_{occ} presented in the experiment at an initial velocity of 10 km/h.

Table III — The estimated fixed effects parameters of the model predicting the TTCs estimates for the accelerating ICEV (internal combustion engine vehicle), EV (electric vehicle without AVAS) and EV+AVAS (electric vehicle with AVAS) at an initial velocity of 10 km/h. Given are effect estimates (β), standard erorrs (*SE*), degrees of freedom (*df*), *t*- und *p*-values.

	β	*SE*	*df*	*t*	*p*
(Intercept)	0.3608	0.2173	60.2	1.68	.098
TTC	0.8729	0.0419	3725	20.87	< .001
TTC × a_{avg}	0.1914	0.0349	3725	5.48	< .001
ICEV × a_{avg}	−0.0312	0.1076	3725	-0.29	.771
EV × a_{avg}	−0.1907	0.0881	3725	-2.17	.030
EV+AVAS × a_{avg}	−0.0311	0.0881	3725	-0.35	.724
ICEV × TTC × v_{occ}	−0.0071	0.0021	3725	-3.43	<.001
EV × TTC × v_{occ}	0.0029	0.0026	3725	1.12	.262
EV+AVAS × TTC × v_{occ}	−0.0027	0.0027	3725	-1.03	.304

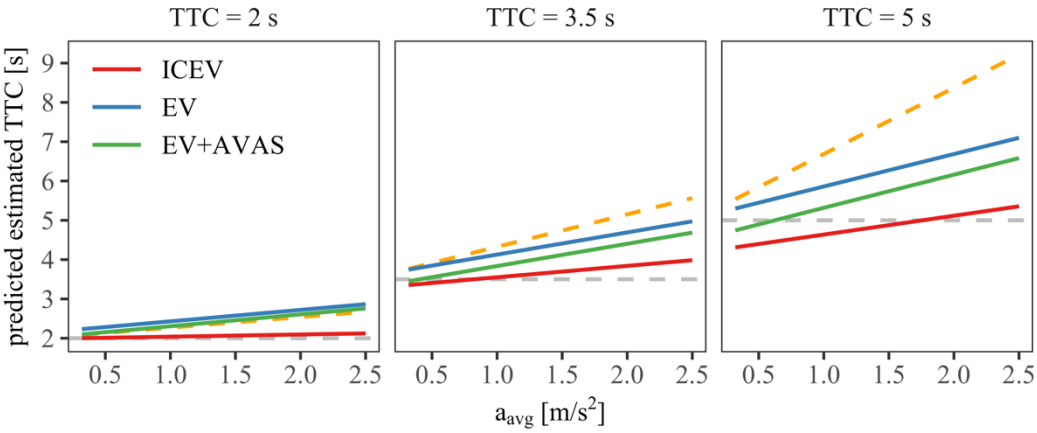

Figure 6 — TTC estimates predicted by the regression model for accelerating ICEV and EV with and without AVAS (*y*-axis) at an initial velocity of 10 km/h as a function of acceleration (x-axis), vehicles types (color coding), and actual TTC (columns). For the prediction, v_{occ} was set to 26.69 km/h. The gray dashed line represents a perfect estimate of the TTC. The yellow dashed line represents the first-order TTC estimate. Color coding: red = ICEV, blue = EV without AVAS, green = EV with AVAS.

The predicted TTC estimates show that as a_{avg} and actual TTC increase, we can expect an increasing overestimation of TTC. The predicted TTC estimates for the EVs again show a pattern similar to a first-order estimation (dashed orange lines), indicating that the acceleration is not adequately considered in the TTC estimation. The model predicts that the TTC for both EVs is significantly overestimated at high acceleration and that this effect becomes stronger as the actual TTC increases. According to the model, the AVAS reduces this effect somewhat, but without reaching the level of TTC estimates for the ICEV. At an acceleration of 2.0 m/s^2 and an actual TTC

of 5.0 s (right panel), the predicted overestimation is about 1.5 for the EV without AVAS, but is reduced to about 1.0 s for the EV with AVAS. In contrast, the predicted TTC estimates for the ICEV show only small deviations from the veridical TTC (dashed gray lines).

At an initial velocity of 20 km/h, all three vehicles were also presented with a lower nominal acceleration of 0.6 m/s². At this acceleration level, the AVAS was still active, at least in the initial phase of the acceleration. As can be seen in Figure 4, for the vehicle approaches with an initial velocity of 20 km/h and a relatively low a_{avg}, the mean estimated TTCs for the EV with and without AVAS were very similar, showing a small amount of TTC overestimation that was slightly more pronounced compared to the ICEV. This pattern was observed for all actual TTCs, with descriptive differences slightly increasing with increasing TTC. Three Bonferroni-corrected pairwise comparisons confirmed that estimated TTCs were significantly shorter for the ICEV than for the EV, $t(89) = 6.00$, $p_{Bonf} < .001$, $d_z = 1.10$, and EV with AVAS, $t(89) = 5.69$, $p_{Bonf} < .001$, $d_z = 1.04$. In contrast, mean TTC estimates for the EV with and without AVAS did not differ significantly, $t(89) = 0.\ 22$, $p_{Bonf} = 1.000$. For the accelerated approaches with an initial velocity of 20 km/h, it can thus be concluded that the acceleration of the EV with and without AVAS was slightly less considered in the TTC estimation compared to the ICEV, presumably due to a less salient acoustic signature of the two EVs.

Statistical analyses of the TTC estimates for vehicles at constant velocities

For each combination of participant, vehicle type, nominal constant velocity v_0, actual TTC, and acoustic recording, the TTC estimates for constant-velocity approaches were examined for outliers using Tukey's method (Tukey, 1977), provided that at least 5 trials of each combination were available. Data points that were more than three interquartile ranges below the first or above the third quartile were excluded from further analyses. Following this procedure, 5 trials of the 7539 constant-velocity approaches were excluded, and a total of 7534 trials were included in the data analyses. Differences in mean estimated TTCs were analyzed using two repeated-measures ANOVAs (multivariate approach). The first rmANOVA considered the constant-velocity approaches of the ICEV and EV without AVAS at all velocities (10-50 km/h). The second rmANOVA additionally considered the EV with AVAS. However, since the AVAS was only active at velocities below 28 km/h, only data at v_0 = 10 and 20 km/h were analyzed in the second rmANOVA.

The mean TTC estimates for the constant-velocity approaches of all vehicle types are shown as a function of the actual TTC in Figure 7. Data points on the diagonal correspond to a perfect TTC estimate. At all velocities v_0, the mean TTC estimates were quite close to the actual TTCs. This confirms that the simulation quality of the VR system was high and that the participants were able to perform the TTC estimation task well. Only at the lowest v_0, the mean TTC estimates showed a more significant deviation from the actual TTC, that is, the TTC was underestimated on average. In addition, across all v_0, the longest actual TTC of 5.0 s was more likely to be underestimated on average than the two shorter TTCs of 2.0 s and 3.5 s. In summary, the descriptive differences between the vehicle types were quite small for the constant-velocity approaches.

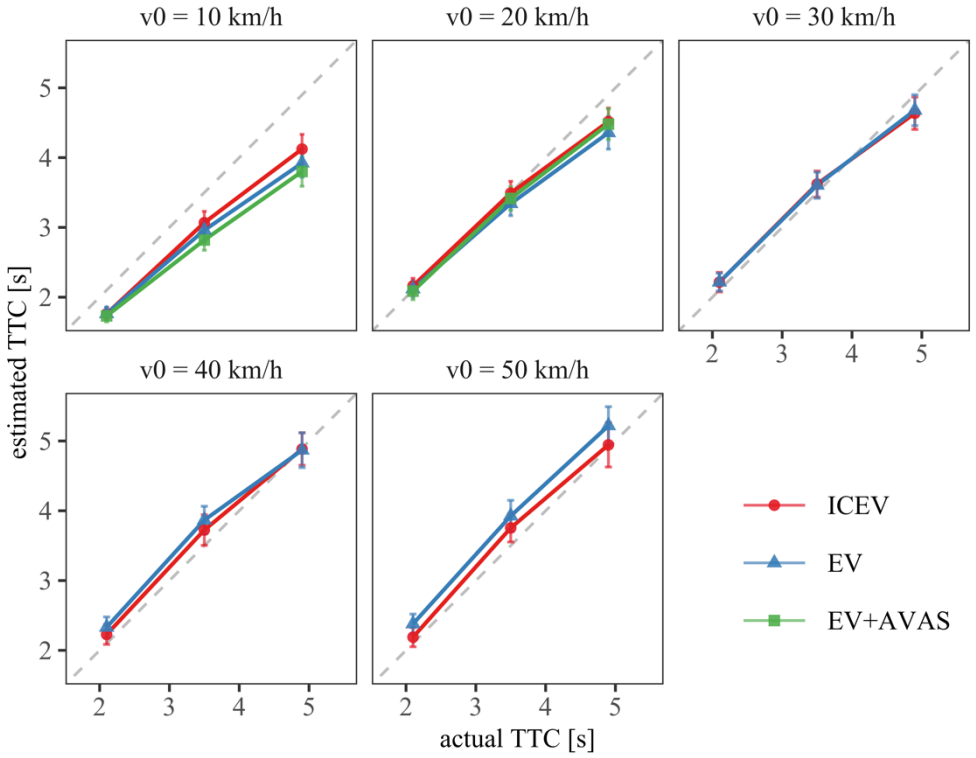

Figure 7 — Mean TTC estimates for vehicles travelling at a constant velocity v_0 (y-axis) as a function of actual TTC (x-axis). Each panel represents a nominal constant velocity v_o. The colors indicate the vehicle type: red = ICEV, blue = EV without AVAS, green = EV with AVAS. The gray dashed line represents a perfect estimate of the TTC. Error bars represent ± 1 SE of the mean.

The first rmANOVA analyzed the TTC estimates for the ICEV and EV without AVAS. It showed no significant difference in the mean estimated TTC between ICEV (M = 3.42 s, SD = 1.48 s) and EV (M = 3.44 s, SD = 1.48 s), $F(1,29) = 0.68$, $p = .417$. Thus, at constant velocities, the different acoustic signatures of ICEV and EV without AVAS did not play a significant role in the mean TTC estimate. However, the interaction between v_0 and vehicle type was significant, $F(4,26) = 10.29$, $p < .001$, $\eta_p^2 = 0.61$. At a v_0 of 10 km/h, the TTC of the EV was on average estimated to be shorter than the TTC of the ICEV. At a v_0 of 40 km/h and higher, this effect reversed (Figure 7), so here, on average, the EV was estimated to arrive later at the participant's position than the ICEV.

The estimated TTC increased significantly with the actual TTC, $F(2,28) = 173.77$, $p < .001$, $\eta_p^2 = 0.93$. Thus, the participants adjusted their TTC estimate to the actual TTC presented (Figure 7). Furthermore, the main effect of velocity was significant, $F(4,26) = 10.75$, $p < .001$, $\eta_p^2 = 0.62$. On average, participants underestimated the TTC at a v_0 = 10 km/h, whereas the TTC was frequently overestimated at the higher speeds. This is compatible with a size-arrival effect (DeLucia, 1991). The size-arrival effect states that for the same actual TTC, an object subtending a larger visual angle is perceived to arrive earlier at a defined position than an object with a smaller visual angle. Since in the present experiment, the vehicle was closer to the participants at 10 km/h than at higher velocities for a given TTC, it corresponded to a larger visual angle on the retina than vehicles at higher velocities. Alternatively, the mean TTC estimates increasing with speed reflect a distance bias. When the vehicle was farther away at occlusion, the TTC was estimated to be longer (Law et al., 1993). Because the size of the simulated vehicle was constant in the experiment, our data do not allow us to differentiate to what extent the effect of velocity is due to its optical size or distance at occlusion. Moreover, the effect of actual TTC interacted with v_0, $F(8,22) = 2.60$, $p = .036$, $\eta_p^2 = 0.49$. At higher velocities the mean estimated TTC increased by almost the same amount as the actual TTC, while at a low v_0 of 10 km/h, the estimated TTC

increased by only about 2 s for a change in actual TTC of 3.0 s (increase from 2.0 to 5.0 s) (Figure 7). In this respect, the TTC estimates were less accurate at the lower constant velocities. Neither the interaction between actual TTC and vehicle type was significant, $F(2,28) = 1.19$, $p = .321$, nor the interaction between actual TTC, v_0 and vehicle type, $F(8,22) = 0.98$, $p = .478$. Thus, the vehicle type did not have a substantial effect in the interaction with the actual TTC and velocity.

The second rmANOVA analyzed the TTC estimates for the constant-velocity approaches with v_0 = 10 and 20 km/h, for all of the three vehicles types (ICEV, EV, EV+AVAS). The mean TTC estimates differed significantly between the vehicle types, $F(2,28) = 13.56$, $p < .001$, $\eta_p^2 = .492$. They were shorter for the EV with AVAS (M = 3.06 s, SD = 1.31 s) and the EV without AVAS (M = 3.08 s, SD = 1.30 s) than for the ICEV (M = 3.19 s, SD = 1.32 s). Subsequent Bonferroni-corrected pairwise comparisons showed that the differences in mean estimated TTCs were significant for the comparison of the ICEV and EV without AVAS, $t(179) = 4.40$, $p_{bonf} < .001$, $d_z = 0.80$ (Cohen, 1988), and for the comparison of the ICEV and EV with AVAS, $t(179) = 4.68$, $p_{bonf} < .001$, $d_z = 0.85$. The mean TTC estimates for the EV and EV with AVAS did not differ significantly, $t(179) = 0.73$, p_{bonf} = 1.000. Thus, the differences between the TTC estimates for ICEV versus EV with and without AVAS, respectively, were more systematic than the difference between the EV with and without AVAS. The effect of vehicle type became more prominent with increasing actual TTC, as indicated by a significant interaction between the actual TTC and vehicle type, $F(4,26) = 5.23$, $p = .003$, η_p^2 = .446. At a TTC of 5.0 s, the largest differences between TTC estimates for the three vehicle types were evident. With increasing actual TTC, participants descriptively underestimated the TTC the most for the EV with AVAS, although descriptive underestimation of TTC for the EV without AVAS was also stronger than for the ICEV. The effect of vehicle type also differed significantly between the two constant velocities, $F(2,28) = 6.60$, $p = .004$, $\eta_p^2 = .320$, with the difference between the estimated TTCs for the three vehicle types being more pronounced at v_0 = 10 km/h than at 20 km/h, as also shown in Figure 7.

The mean TTC estimates increased with increasing actual TTC, $F(2,28) = 148.63$, $p < .001$, η_p^2 = .914, indicating that participants adjusted their TTC estimates according to the presented actual TTC. In addition, the mean TTC estimates increased from v_0 = 10 to 20 km/h, $F(1,29) = 62.62$, $p <$ .001, $\eta_p^2 = .683$. This is again compatible with a size-arrival effect or distance bias. Neither the interaction between v_0 and actual TTC, $F(2,28) = 3.03$, $p = .064$, nor the three-way interaction between vehicle type, actual TTC, and v_0 were significant, $F(4,26) = 2.20$, $p = .097$.

Overall, there was no substantial effect of vehicle type at most constant velocities. Even at the lowest v_0, where there was a significant effect of vehicle type, the differences between the mean TTC estimates for ICEV and the two EVs were rather small. Also, the AVAS had no significant effect on the TTC estimates. This pattern is compatible with previous studies that found no substantial (or no particularly large) differences between mean TTC estimates in a purely visual and an audiovisual presentation for objects moving at constant speed (DeLucia et al., 2016; Keshavarz & Hecht, 2011; Wessels et al., under review; Zhou et al., 2007).

Discussion

In the present study, we investigated whether TTC estimates for accelerating vehicles differ between vehicles with an internal combustion engine (ICEVs) and electric vehicles (EVs) with and without AVAS, from a pedestrian's point of view. For accelerated vehicle approaches, the data indicated a strong systematic difference in TTC estimation between the three vehicle types. As hypothesized, the TTC estimates for the EVs with and without AVAS showed a pattern compatible with first-order TTC estimation (Lee et al., 1983), indicating that the EVs' acceleration was not adequately taken into account during estimation. The results showed an overestimation of the TTC, which increased with longer actual TTC, stronger acceleration, and lower velocity at the moment of estimation. Such first-order patterns have been previously reported for TTC estimation of accelerating objects based only on visual information (e.g., Benguigui et al., 2003;

Benguigui & Bennett, 2010; Bennett & Benguigui, 2016; Kaiser & Hecht, 1995; Lee et al., 1983; Rosenbaum, 1975; Senot et al., 2003). In the present experiment, the TTC estimations for accelerating EVs lay between the first-order TTC and the actual TTC in most cases (see Figure 5 and Figure 6), which suggests that the acceleration might have been partly, but by no means completely been considered during estimation. In contrast, for the accelerating ICEV, there was only a weak tendency towards a first-order pattern in the TTC estimates. Thus, on average significantly more accurate estimations were observed, compared to the accelerating EVs. This is compatible with results from a previous study from our lab (Wessels et al., under review) in which the mean TTC estimations for an accelerating vehicle showed a clear first-order pattern in a visual-only condition (without vehicle sound), but were largely accurate when the sound of an accelerating ICEV was added. In the present study, the AVAS mitigated the extent of TTC overestimation observed for the accelerating EV without AVAS. However, it did not result in the same level of accuracy as for the ICEV on average. In sum, the altered sound of an accelerating EV without AVAS substantially impaired pedestrians' TTC judgments compared to the sound of an accelerating ICEV, and was improved only to a limited extent when the AVAS of the EV was activated.

Why does the sound of an ICEV provide a better basis to accurately judge the TTC during accelerating vehicle approaches than the sound of an EV (with and without AVAS)? In our previous study (Wessels et al., under review), we supposed that the sound of an ICEV enables humans to correct for visual TTC estimation errors, i.e., the first-order pattern. In the following, we outline possible reasons why this "audiovisual benefit" of the vehicle sound was reduced for EVs with and without AVAS in comparison to the ICEV. In the present study, the sound of all three vehicle types provided spatial information about the vehicle's distance, velocity and acceleration through the dynamic spatial sound field generated during the approach. That is, changes in interaural time and level differences delivered information about, e.g., the changing lateral angle between the left curb where the observer was standing in the virtual scene and the right front tire. However, as explained in the method section, the trajectories of the ICEV and EV with and without AVAS recorded on the test track and presented in the experiment differed to a certain extent. We addressed this problem in the data analysis by using regression models in which the actual acceleration and the actual speed at occlusion were entered as continuous predictors. These regression models were used to predict TTC estimations for the three vehicles at exactly the same acceleration and velocity (see Figure 5 and Figure 6). Since they confirmed the differences in the patterns of TTC estimates among the three vehicle types, the effect of vehicle type can be attributed to the different acoustic signatures of the vehicle types. Notwithstanding that additional experiments would be desirable in which the vehicle types have identical trajectories i.e., differ only in terms of sound, to further confirm the results of the present experiment, our analyses indicate that differences in trajectories are not a likely explanation for the strong differences in TTC estimates between the three vehicle types.

Rather, we suggest that the more accurate TTC estimations for accelerating ICEVs compared to accelerating EVs were driven by the specific sound profiles of the accelerating vehicles. The sound of an accelerating ICEV conveys characteristic acceleration cues. The frequencies of the harmonic components of the powertrain noise rise linearly with the rotational speed of the engine. In the present study, the sound profile of the accelerating ICEV also provided additional signals about the acceleration due to gear shifts sometimes performed during the approach (see Table I), which resulted in a characteristic pattern of increasing frequency followed by a transient drop in frequency during the gear shift. In addition, the sound level of the powertrain noise increases by approximately 12 dB per doubling of the rotational speed and also depends on the engine load (Zeller, 2018). Therefore, the acceleration of the ICEV was presumably easy for the participants to recognize, which may have helped them to consider the acceleration in their TTC estimation, thus correcting for visual TTC estimation errors. In contrast, the accelerating EV without AVAS mostly lacks the aforementioned acceleration cues associated with an ICEV. The powertrain noise is substantially quieter than for an ICEV, does not exhibit the same characteristic harmonic sound spectrum as a combustion engine, and is also less likely familiar to participants. Conform with

European legislation (UNECE R138, 2017), the AVAS sound must include an increase in the frequency of at least one frequency component by at least 0.8% per increase in speed by 1 km/h in the range from 5 to 20 km/h, to communicate the dynamic driving behavior to pedestrians. However, the dynamic changes in the AVAS sound spectrum during acceleration presented in our experiment were still more subtle than for the ICEV. Accordingly, the participants might either not have recognized at all when the EVs were accelerating, or might have noticed that the EVs were accelerating but underestimated the level of acceleration. In both cases, participants would not have been able to correct for visual estimation errors, or at least not sufficiently. To measure whether and to what extent the sound of accelerating EVs allows for the correction of visual TTC estimates, it would be interesting to include a visual-only in addition to an audiovisual vehicle presentation in future studies. With this approach, it would be possible to investigate whether the sound of accelerating EVs provides a significant audiovisual benefit, as observed for an accelerating ICEV in a previous study from our lab (Wessels et al., under review).

On a more general level, the exact auditory cues and mechanisms involved in TTC estimation for accelerating vehicles remain to be identified. For instance, due to the dependence of the powertrain noise level on the rotational speed, the loudness of the accelerating ICEV at occlusion was higher than for the EVs. For constant-velocity approaches, participants tend to judge softer vehicles and other sound sources to arrive later than louder sound sources at the same actual TTC (DeLucia et al., 2016; Keshavarz et al., 2017; Oberfeld et al., under review), described by the so-called *intensity-arrival effect* (DeLucia et al., 2016). This effect might partly be responsible for the shorter TTC estimates for accelerating ICEVs compared to EVs, but additional experiments are required to test this hypothesis, ideally including conditions presenting all vehicle types at identical loudness at occlusion (see Oberfeld et al., under review). The reliance of pedestrians on dynamic spectral and pitch cues during TTC estimation should also be investigated. In addition to such experiments on TTC estimation, it would be interesting to examine the auditory and audiovisual sensitivity for detecting whether an approaching object is accelerating for the three vehicle types. If the acceleration sensitivity is significantly worse for an EV than for an ICEV, as we would expect, this would imply that participants in the present experiment mostly lacked access to acceleration information for the EVs, simply because they did not realize that the vehicles were accelerating. If, however, the acceleration detection sensitivities do not differ between vehicle types to a large extent, this would rather support the argument that the EVs' state of acceleration was perceived in the present study but that the level of acceleration was comparatively underestimated. As a consequence, participants could have incorporated information about the EVs' acceleration, in their TTC estimation, but to a smaller extent than optimal.

Did the activated AVAS remove the first-order pattern in the TTC estimation for the accelerating EV, as one might have guessed? The answer is no – in fact, the TTC estimates for the accelerating EV with AVAS were similar to the TTC estimates for the EV without AVAS, and also showed a first-order pattern, only to a slightly lesser extent. In Figure 6, the predicted estimated TTC for the EV with and without AVAS both increase with increasing acceleration, but the predicted estimations for the EV with AVAS are constantly shifted towards lower predicted overestimations. In sum, the acceleration for the EV with AVAS was slightly more adequately taken into account than for the EV without AVAS. However, the TTC estimates of the accelerating EV with AVAS were still significantly less accurate than for the ICEV, suggesting that the amount of frequency shift in the presented AVAS as a function of velocity might not have been sufficiently strong, or not the only relevant acoustic cue to convey the accelerating state. First, to give an example, if an ICEV increases its speed from 10 km/h to 20 km/h without shifting gears, the rotational speed of the engine increases by a factor of 2 (100%), and so does the fundamental frequency of the harmonic components of the powertrain noise. In contrast, UNECE R138 (2017) requires only a frequency increase by 0.8% per 1 km/h, that is, $(1.008^{10} - 1) \cdot 100 = 8.29$ % across the same change in speed. Second, the sound level of an ICEV increases strongly with the rotational speed and load (Zeller, 2018), while the European AVAS regulation (in contrast to the US-American AVAS regulation NHTSA 141) does not require an increase in sound level with increasing speed. Third,

all presented acoustic recordings of the ICEV accelerating from an initial velocity of 10 km/h also included a clearly noticeable gear shift. As outlined before, it is conceivable that the gear shift served as acceleration signal which the participants were probably very familiar with. Hence, this ICEV-specific acceleration signal could have contributed to the detection of acceleration, but also to the correct representation of the acceleration level during estimation.

The prerequisite for a potential influence of the gear shift as an informative cue would be the knowledge of how to interpret it. Accordingly, this could mean that as participants become more familiar with the AVAS sounds and learn how to access the AVAS-specific acoustic acceleration cues, their estimates might become substantially more accurate, or even as accurate as for the commonly encountered ICEV. In this context, it might be beneficial to adapt the AVAS design towards a more ICEV-like concept, so that road users do not have to learn "from the scratch" how to interpret the AVAS sound profile to accurately estimate the TTC of an accelerating EV. Furthermore, road users are currently confronted with AVAS sounds from different car manufacturers that designed their individual AVAS sound profiles. The European legislation mandates AVAS designers to comply with certain standards, such as a sound level of between 56 dB(A) and 75 dB(A) at 20 km/h and under certain measurement conditions, and a minimal frequency shift of 0.8% for at least one frequency component per 1 km/h during acceleration. Nonetheless, it leaves a lot of room to create different branding sounds. Consequently, it might be quite difficult for road users to get familiar with "the" sound profile of an EV with AVAS, because AVAS sounds show an even larger variability than those of an ICEV. If there were a uniform AVAS variant, or at least less variability between the different AVAS sound profiles, then it might be easier for road users to become familiar with "the" sound profile of an EV with AVAS.

In sum, the findings suggest that the acoustic signature of accelerating EVs lacks salient information to estimate the TTC as accurately as for ICEVs, which the AVAS – at least in the variant studied here – can only partly compensate for. Further research is needed to determine on which (combination of) auditory cues in the sound profile pedestrians rely to accurately estimate the TTC of an accelerating vehicle, or whether the human perception can adapt to the "new" sound profile of an accelerating EV with AVAS. From a perspective of traffic safety, the TTC overestimations, observed particularly for the EVs accelerating from a low initial velocity, could lead to risky crossing behavior of pedestrians in a real traffic situation. Thus, we conclude that in the case of accelerated vehicle approaches, the altered acoustic signatures of EVs with and without AVAS could pose a potential collision risk to pedestrians.

For vehicles traveling at a constant speed, the acoustic signature of the vehicle types played only a minor role in the present study, in line with our expectations. We observed similar TTC estimates for the ICEV and EV with and without AVAS at most constant velocities, which were quite close to the veridical TTC values. Even at the lowest constant velocity, where the effect of vehicle type reached significance, the differences regarding the mean TTC estimates were rather small. This finding is consistent with previous studies that have found no significant (or no particularly large) benefit of additional auditory information in an audiovisual presentation over purely visual representations of object approaches at constant velocities (DeLucia et al., 2016; Hassan, 2012; Keshavarz et al., 2017; Schiff & Oldak, 1990; Wessels et al., under review; Zhou et al., 2007).

In the present experiment, we presented the sounds of one specific ICEV and one specific EV (with and without activated AVAS). This limits the generalizability of the findings to different models of ICEVs, EVs, and AVAS designs. Assuming that our perception is sensitive to the acoustic signatures of vehicles, it is conceivable that auditory differences between different vehicle models, also of the same vehicle type, could be relevant. Even ICEVs can differ significantly in their powertrain noise, due to differences in motorization and sound design. This is even more relevant for the numerous different AVAS designs. For future research, it would therefore be desirable to investigate a larger number of various models of ICEVs, EVs with and without AVAS to increase the ecological validity of the data.

For the three vehicle models used here, we presented acoustic recordings of *real* vehicles and simulated exactly the same trajectories as during the drives on the test track. While this exact match between vehicle sounds and trajectories resulted in high ecological validity, the trajectories during acceleration partly deviated from the intended driving profiles, and differed between the vehicle types. In addition, some driving conditions required to shift gears for the ICEV, which led to further differences in driving dynamics (drop in acceleration when the gear shift is initiated, followed by a stronger acceleration for a short period). Even though we were able to identify effects of the vehicle sound on TTC estimates by statistically controlling for the differences in trajectories, it would be desirable to achieve higher experimental control in future investigations by presenting identical driving profiles for all vehicle types, as mentioned before.

Furthermore, the traffic scenarios used in the experiments were presented using realistic audiovisual simulations. The relatively accurate TTC estimates for the constant-velocity approaches, even compared to previous studies (DeLucia et al., 2016; Hassan, 2012; Keshavarz et al., 2017; Schiff & Oldak, 1990; Zhou et al., 2007), confirm the high quality of the sensory information presented in the simulations. Based on previous studies, we assume that in the traffic scenario we presented, TTC estimation provides the basis of pedestrians' road-crossing behavior (e.g., Lee et al., 1984; Petzoldt, 2014). However, to gain a deeper understanding of pedestrians' behavior in interaction with the different vehicle types, it would be interesting to directly investigate road-crossing decisions in the same experimental conditions.

In terms of sample characteristics, the requirements for participation in the present study were normal hearing and (corrected-to-)normal vision, which ensured that the participants were able to fully perceive the presented auditory and visual information. In turn, it is unclear to what extent the findings can be transferred to groups with visual or auditory impairments. For instance, when vision is impaired, auditory information might play an even more important role than suggested in the present study. Thus, the different sounds of the vehicle types might have an even stronger effect on TTC estimation than for normally sighted people. However, no data are yet available regarding the relative weighting of auditory and visual cues during TTC estimation for (accelerated) vehicle approaches, and how visual impairment affects this weighting. In the same line of reasoning, hearing impairment reduces not only the detectability of sound sources due to elevated thresholds, but also negatively affects auditory localization abilities (e.g., Füllgrabe & Moore, 2018). Even when impaired hearing is compensated with hearing aids, limitations of spatial localization of sound sources are often encountered (for a review, see Akeroyd & Whitmer, 2016). In addition, the processing of dynamic intensity changes may be altered by multichannel compression, which is an important feature of the hearing aid signal processing algorithms optimized for speech intelligibility. The consequences of hearing impairment and hearing aids for the perception of approaching vehicles have not been experimentally investigated yet. Such data would be helpful for assessing traffic risks associated with, e.g., aging.

Finally, the presented diffuse spatial background sound recorded in a residential area was relatively quiet with 37.5 dB(A). A louder background sound as often experienced in city centers could interfere with the use of the vehicle sound. That is, if the background sound is so loud that it almost masks the vehicle sound, then of course pedestrians will not benefit much from it during TTC estimation. Nonetheless, the powertrain noise of accelerating ICEVs is on average louder than for EVs, and thus presumably easier to perceive even with louder background sound. Further experiments on the audiovisual benefit for accelerating ICEVs and EVs with and without active AVAS would be relevant to investigate whether the effect of vehicle type is amplified in loud background noise.

Conclusions

The present study showed that the sound of an accelerating conventional ICEV provides salient information that enables pedestrians to judge its TTC rather accurately. When an EV accelerated from a low initial velocity, the TTC estimates were substantially more erroneous compared to the ICEV, and more similar to a first-order TTC estimation pattern, indicating that the acceleration was not sufficiently considered during estimation. The AVAS slightly reduced the first-order pattern, but it did not enable the participants to estimate the TTCs as accurately as for the accelerating ICEV. We conclude that the acoustic signature of accelerating EVs lacks salient information to assess TTC as accurately as for ICEVs, which the AVAS can only partly compensate for. This suggests a potentially higher collision risk when pedestrians interact with EVs without and with AVAS. Our results highlight the importance of gaining a better understanding of the role of auditory perception in ensuring traffic safety. This requires an expansion of the research focus on auditory detection that dominated so far to studies of road-crossing decisions and other scenarios involving judgments of vehicle motion.

Acknowledgements

This work was supported by funding from German Insurers Accident Research (Unfallforschung der Versicherer, udv.de) granted to author DO. Author SK is an employee of the funding agency and was involved in the design of the study, but there were no conflicts of interest.

We are grateful to Giso Grimm (Medical Physics, Uni Oldenburg) for his help in implementing the acoustic simulations in TASCAR, to Agnes Münch (Experimental Psychology, Uni Mainz) for her support in implementing the visual VR simulations, and to Vanessa Dimmler for her assistance in data collection.

References

Ahrens, J., Rabenstein, R., & Spors, S. (2014). Sound field synthesis for audio presentation. *Acoustics Today*, *10*(2), 15–25.

Akeroyd, M. A., & Whitmer, W. M. (2016). Spatial hearing and hearing aids. In *Hearing Aids* (Vol. 56, pp. 181–215).

Allen, J. B., & Berkley, D. A. (1979). Image Method for Efficiently Simulating Small-room Acoustics. *Journal of the Acoustical Society of America*, *65*(4), 943–950.

Bach, M. (1996). The Freiburg Visual Acuity Test-automatic measurement of visual acuity. *Optometry and Vision Science*, *73*(1), 49–53. https://doi.org/10.1097/00006324-199601000-00008

Belsey, D. A., Kuh, E., & Welsch, R. E. (2005). *Regression diagnostics: Identifying influential data and sources of collinearity*. John Wiley & Sons.

Benguigui, N., & Bennett, S. J. (2010). Ocular pursuit and the estimation of time-to-contact with accelerating objects in prediction motion are controlled independently based on first-order estimates. *Experimental Brain Research*, *202*(2), 327–339. https://doi.org/10.1007/s00221-009-2139-0

Benguigui, N., Ripoll, H., & Broderick, M. P. (2003). Time-to-Contact Estimation of Accelerated Stimuli Is Based on First-Order Information. *Journal of Experimental Psychology: Human Perception and Performance*, *29*(6), 1083–1101. https://doi.org/10.1037/0096-1523.29.6.1083

Bennett, A. G., & Rabbetts, R. B. (1998). *Clinical visual optics* (3rd ed.). Butterworth-Heinemann.

Bennett, S. J., & Benguigui, N. (2016). Spatial Estimation of Accelerated Stimuli Is Based on a Linear Extrapolation of First-Order Information. *Experimental Psychology*, *63*(2), 98–106. https://doi.org/10.1027/1618-3169/a000318

Cohen, J. (1988). *Statistical power analysis for the behavioral sciences* (2nd ed). L. Erlbaum Associates.

DeLucia, P. R. (1991). Pictorial and Motion-Based Information for Depth Perception. *Journal of Experimental Psychology: Human Perception and Performance*, *17*(3), 738–748.

DeLucia, P. R., Preddy, D., & Oberfeld, D. (2016). Audiovisual Integration of Time-to-Contact Information for Approaching Objects. *Multisensory Research*, *29*(4–5), 365–395. https://doi.org/10.1163/22134808-00002520

Füllgrabe, C., & Moore, B. C. J. (2018). The Association Between the Processing of Binaural Temporal-Fine-Structure Information and Audiometric Threshold and Age: A Meta-Analysis. *Trends in Hearing*, *22*, 233121651879725. https://doi.org/10.1177/2331216518797259

Gergen, S., Grautstuck, C., & Martin, R. (2012). *Messtechnische Untersuchung der Akustik eines Elektroautos*. 2.

Gordon, C. C., Churchill, T., Clauser, C. E., Bradtmiller, B., McConville, J. T., Tebbetts, I., & Walker, R. A. (1989). *Anthropometric survey of US Army personnel: Summary statistics, interim report for 1988*. Anthropology Research Project Inc Yellow Springs OH.

Gottsdanker, R., Frick, J. W., & Lockard, R. (1961). Identifying the acceleration of visual targets. *British Journal of Psychology*, *52*(1), 31–42.

Grimm, G., Luberadzka, J., & Hohmann, V. (2019). A Toolbox for Rendering Virtual Acoustic Environments in the Context of Audiology. *Acta Acustica United with Acustica*, *105*(3), 566–578. https://doi.org/10.3813/AAA.919337

Hassan, S. E. (2012). Are Normally Sighted, Visually Impaired, and Blind Pedestrians Accurate and Reliable at Making Street Crossing Decisions? *Investigative Opthalmology & Visual Science*, *53*(6), 2593. https://doi.org/10.1167/iovs.11-9340

Hofbauer, M., Wuerger, S. M., Meyer, G. F., Roehrbein, F., Schill, K., & Zetzsche, C. (2004). Catching audiovisual mice: Predicting the arrival time of auditory-visual motion signals. *Cognitive, Affective, & Behavioral Neuroscience*, *4*(2), 241–250. https://doi.org/10.3758/CABN.4.2.241

International Transport Forum. (2012). *Pedestrian Safety, Urban Space and Health*. OECD. https://doi.org/10.1787/9789282103654-en

Ishaque, M. M., & Noland, R. B. (2008). Behavioural Issues in Pedestrian Speed Choice and Street Crossing Behaviour: A Review. *Transport Reviews*, *28*(1), 61–85. https://doi.org/10.1080/01441640701365239

ISO 9613-2:1999-10. (1999). *Acoustics—Attenuation of sound during propagation outdoors—Part 2: General method of calculation.*

James, G., Witten, D., Hastie, T., & Tibshirani, R. (2013). *An introduction to statistical learning* (Vol. 112). Springer.

Jenison, R. L. (1997). On Acoustic Information for Motion. *Ecological Psychology*, *9*(2), 131–151. https://doi.org/10.1207/s15326969eco0902_2

Kaiser, M. K., & Hecht, H. (1995). Time-to-passage judgments in nonconstant optical flow fields. *Perception & Psychophysics*, *57*(6), 817–825. https://doi.org/10.3758/BF03206797

Kenward, M. G., & Roger, J. H. (1997). Small Sample Inference for Fixed Effects from Restricted Maximum Likelihood. *Biometrics*, *53*(3), 983. https://doi.org/10.2307/2533558

Keshavarz, B., Campos, J. L., DeLucia, P. R., & Oberfeld, D. (2017). Estimating the relative weights of visual and auditory tau versus heuristic-based cues for time-to-contact judgments in realistic, familiar scenes by older and younger adults. *Attention, Perception, & Psychophysics*, *79*(3), 929–944. https://doi.org/10.3758/s13414-016-1270-9

Keshavarz, B., & Hecht, H. (2011). Validating an Efficient Method to Quantify Motion Sickness. *Human Factors: The Journal of the Human Factors and Ergonomics Society*, *53*(4), 415–426. https://doi.org/10.1177/0018720811403736

Kropp, W., Sabiniarz, P., Brick, H., & Beckenbauer, T. (2012). On the sound radiation of a rolling tyre. *Journal of Sound and Vibration*, *331*(8), 1789–1805. https://doi.org/10.1016/j.jsv.2011.11.031

Law, D. J., Pellegrino, J. W., Mitchell, S. R., Fischer, S. C., McDonald, T. P., & Hunt, E. B. (1993). Perceptual and Cognitive Factors Governing Performance in Comparative Arrival-Time Judgments. *Journal of Experimental Psychology: Human Perception and Performance*, *19*(6), 1183–1199.

Lee, D. N., Young, D. S., & Mclaughlin, C. M. (1984). A roadside simulation of road crossing for children. *Ergonomics*, *27*(12), 1271–1281. https://doi.org/10.1080/00140138408963608

Lee, D. N., Young, D. S., Reddish, P. E., Lough, S., & Clayton, T. M. H. (1983). Visual Timing in Hitting An Accelerating Ball. *The Quarterly Journal of Experimental Psychology Section A*, *35*(2), 333–346. https://doi.org/10.1080/14640748308402138

Nakagawa, S., & Schielzeth, H. (2013). A general and simple method for obtaining R^2 from generalized linear mixed-effects models. *Methods in Ecology and Evolution*, *4*(2), 133–142. https://doi.org/10.1111/j.2041-210x.2012.00261.x

NHTSA 141. (2018). *Federal Motor Vehicle Safety Standard No. 141: Minimum Sound Requirements for Hybrid and Electric Vehicles*.

Oberfeld, D., Wessels, M., & Büttner, D. (under review). *Overestimated time-to-collision for quiet vehicles: Evidence from a study using a novel audiovisual virtual-reality system for traffic scenarios*.

Parizet, E., Ellermeier, W., & Robart, R. (2014). Auditory warnings for electric vehicles: Detectability in normal-vision and visually-impaired listeners. *Applied Acoustics*, *86*, 50–58. https://doi.org/10.1016/j.apacoust.2014.05.006

Petzoldt, T. (2014). On the relationship between pedestrian gap acceptance and time to arrival estimates. *Accident Analysis & Prevention*, *72*, 127–133. https://doi.org/10.1016/j.aap.2014.06.019

Poveda-Martínez, P., Peral-Orts, R., Campillo-Davo, N., Nescolarde-Selva, J., Lloret-Climent, M., & Ramis-Soriano, J. (2017). Study of the effectiveness of electric vehicle warning sounds depending on the urban environment. *Applied Acoustics*, *116*, 317–328. https://doi.org/10.1016/j.apacoust.2016.10.003

Prime, S. L., & Harris, L. R. (2010). Predicting the position of moving audiovisual stimuli. *Experimental Brain Research*, *203*(2), 249–260. https://doi.org/10.1007/s00221-010-2224-4

Rosenbaum, D. A. (1975). Perception and Extrapolation of Velocity and Acceleration. *Journal of Experimental Psychology: Human Perception and Performance*, *1*(4), 395–403. https://doi.org/10.1037/0096-1523.1.4.395

Schiff, W., & Detwiler, M. L. (1979). Information used in judging impending collision. *Perception*, *8*(6), 647–658.

Schiff, W., & Oldak, R. (1990). Accuracy of Judging Time to Arrival: Effects of Modality, Trajectory, and Gender. *Journal of Experimental Psychology: Human Perception and Performance*, *16*(2), 303–316.

Senot, P., Prévost, P., & McIntyre, J. (2003). Estimating time to contact and impact velocity when catching an accelerating object with the hand. *Journal of Experimental Psychology: Human Perception and Performance*, *29*(1), 219–237. https://doi.org/10.1037/0096-1523.29.1.219

Snowden, R. J., & Braddick, O. J. (1991). The temporal integration and resolution of velocity signals. *Vision Research*, *31*(5), 907–914. https://doi.org/10.1016/0042-6989(91)90156-Y

Statistisches Bundesamt. (2021). *Verkehr: Verkehrsunfälle 2020*. https://www.destatis.de/DE/Themen/Gesellschaft-Umwelt/Verkehrsunfaelle/Publikationen/Downloads-Verkehrsunfaelle/verkehrsunfaelle-jahr-2080700207004.pdf?__blob=publicationFile

Tresilian, J. R. (1995). Perceptual and cognitive processes in time-to-contact estimation: Analysis of prediction-motion and relative judgment tasks. *Perception & Psychophysics*, *57*(2), 231–245. https://doi.org/10.3758/BF03206510

Tukey, J. W. (1977). Exploratory Data Analysis. *Reading, Mass.: Addison-Wesley Pub. Co.*

UNECE R138. (2017). *Regelung Nr. 138 der Wirtschaftskommission für Europa der Vereinten Nationen (UNECE)—Einheitliche Bestimmungen für die Genehmigung geräuscharmer Straßenfahrzeuge hinsichtlich ihrer verringerten Hörbarkeit*.

Watamaniuk, S. N. J., & Heinen, S. J. (2003). Perceptual and oculomotor evidence of limitations on processing accelerating motion. *Journal of Vision*, *3*(11), 5. https://doi.org/10.1167/3.11.5

Werkhoven, P., Snippe, H. P., & Alexander, T. (1992). Visual processing of optic acceleration. *Vision Research*, *32*(12), 2313–2329. https://doi.org/10.1016/0042-6989(92)90095-Z

Wessels, M., Zähme, C., & Oberfeld, D. (under review). *Auditory information improves time-to-collision estimation for accelerating vehicles*.

Yarkoni, T., & Westfall, J. (2017). Choosing Prediction Over Explanation in Psychology: Lessons From Machine Learning. *Perspectives on Psychological Science*, *12*(6), 1100–1122. https://doi.org/10.1177/1745691617693393

Zeller, P. (Ed.). (2018). *Handbuch Fahrzeugakustik*. Springer Fachmedien Wiesbaden. https://doi.org/10.1007/978-3-658-18520-6

Zhou, L., Yan, J., Liu, Q., Li, H., Xie, C., Wang, Y., Campos, J. L., & Sun, H. (2007). Visual and Auditory Information Specifying an Impending Collision of an Approaching Object. In J. A. Jacko (Ed.), *Human-Computer Interaction. Interaction Platforms and Techniques* (Vol. 4551, pp. 720–729). Springer Berlin Heidelberg. https://doi.org/10.1007/978-3-540-73107-8_80

Zotter, F., & Frank, M. (2019). *Ambisonics: A Practical 3D Audio Theory for Recording, Studio Production, Sound Reinforcement, and Virtual Reality* (Vol. 19). Springer International Publishing. https://doi.org/10.1007/978-3-030-17207-7